

## Generalized Oscillator Strengths for the Resonance Transitions in Alkaline-Earth Atoms

Yong-Ki Kim\*

*Argonne National Laboratory, Argonne, Illinois 60439*

Paul S. Bagus

*IBM Research Laboratory, Monterey and Cottle Roads, San Jose, California 95193*

(Received 24 May 1973)

The generalized oscillator strengths (GOS), which are essential factors in the Born cross sections, have been calculated for the lowest  $^1P$  transitions in Mg, Ca, Sr, and Ba from the multiconfiguration Hartree-Fock wave functions with two or three configurations each in the ground and the excited states. The optical limits ( $f$  values) of the GOS agree with experimental values to within 12%. Theoretical data on zero minima and subsequent maxima in the GOS are presented. Our data show that the resonance transition in Ba is the most favorable one for experimental study of the extrema. Since the Born cross sections vanish at the minima, the experimental study of the minima would reveal valuable information on the validity of the first Born approximation, as well as on the magnitudes of higher-order effects not included in the theory. Data for the integrated Born cross sections are presented also. Recent electron-impact data on the resonance transition of Ca agree with the integrated cross section to within 5% for incident energies of 250 eV and higher. Our data show that the relativistic effects in the cross section for Ba are minor compared to the correlation effect between the two valence electrons.

### I. INTRODUCTION

The Born cross sections for the helium atom have been evaluated with a variety of wave functions.<sup>1-5</sup> These studies indicate that the Hartree-Fock (HF) wave functions lead to the Born cross sections within 10 to 20% of those obtained from accurate wave functions for discrete dipole-allowed transitions. However, for alkaline-earth atoms, the HF wave functions produce poor optical oscillator strengths ( $f$  values) for the resonance transitions  $[(ns)^2^1S - (nsnp)^1P]$ .<sup>6-8</sup> For instance, the  $f$  value for Ba from the HF wave functions is ~70% larger than the experimental value adopted by Miles and Wiese.<sup>9</sup> Since the  $f$  value is closely related to the generalized oscillator strength (GOS), which in turn is the essential factor in the (first) Born cross section,<sup>10,11</sup> we expect that the HF wave functions would give poor Born cross sections also.

In this paper we present the result of a study on the effectiveness of the multiconfiguration Hartree-Fock (MCHF) wave functions of modest sizes in calculating  $f$  values and Born cross sections for the resonance transitions in the alkaline-earth atoms (Mg, Ca, Sr, and Ba).

The MCHF wave functions are wave functions with electron correlation included through the configuration-interaction (CI) method. The conventional CI method preselects a number of configurations to mix, and then determines mixing coefficients by the variational principle, while keeping the wave functions for the selected configurations fixed. The MCHF method<sup>12</sup> varies

both the mixing coefficients and the wave functions for the selected configurations, thus allowing for more flexibility in the variational procedure. The MCHF calculations were first carried out using two configurations for O, O<sup>+</sup>, and O<sup>++</sup> by Hartree, Hartree, and Swirles.<sup>13</sup> Recently, several MCHF calculations have been performed on the first-row atoms and their isoelectronic sequences,<sup>14,15</sup> and using relativistic wave functions for considerably heavier atoms as well.<sup>16</sup>

As usual, we have chosen the wave functions to be of the HF type, i.e., a linear combination of the Slater determinants, and each determinant is built from nonrelativistic orbitals. The radial part of each orbital is determined numerically by solving coupled integro-differential equations similar to those in the restricted HF method.<sup>17</sup> The angular part is the usual spherical harmonics.

The numerical procedure for the MCHF method is somewhat more involved than that for the (one-configuration) HF method; however, the reward is worthwhile because the MCHF wave functions are only slightly more complicated than the HF wave functions. Indeed, we find that the addition of one more configuration beyond the HF configuration in both the ground ( $^1S$ ) and the excited ( $^1P$ ) states is sufficient to obtain  $f$  values for the resonance transitions which agree with known experimental data within 7%.<sup>8</sup>

The effective charge for the valence shells is a small fraction of the nuclear charge. Therefore, direct relativistic effects on the valence orbitals of heavy atoms are expected to be small. However, relativistic effects will change the charge

distribution in the core and this in turn may significantly change the potential seen by the valence electrons. We have estimated relativistic effects for the resonance transition in Ba and found them to be small. Thus it appears that for the other atoms considered in this paper they are likely to be small as well.

The GOS and therefore the Born cross sections for these resonance transitions show zero minima. The zero minima appear whenever the transition matrix element changes sign at certain values of the momentum transfer. The positions of the minima and the magnitude of the subsequent maxima are sensitive to the details of the wave functions.<sup>18</sup> We present theoretical data on the first minimum and its subsequent maximum. Other extrema occur at larger momentum transfers, and are too difficult to study experimentally.

In the neighborhood of a minimum, the effects not included in the first Born approximation (such as the distortion of the plane waves) dominate. Hence, a careful experimental study of the minima in the GOS would provide a powerful test for more advanced collision theories.

When the incident particle is much faster than the orbital velocities of the atomic electrons, the integrated (over the angles of the scattered electron) Born cross section can be expressed in terms of a few parameters, which are independent of incident energy.<sup>1,10,19</sup> These parameters for the Born cross sections evaluated from the theoretical GOS are presented, and the resulting cross section for Ca is compared with recent experimental data.

## II. WAVE FUNCTIONS

Our goal in the choice of configurations for the MCHF wave functions has been to include, in addition to the HF configuration, the most important leading terms in a complete CI expansion for the wave function. By most important we mean those configurations which enter with large mixing coefficients in the CI expansion. The precise meaning of large is determined, in part, by the properties which will be calculated with the MCHF wave functions; in the present case, oscillator strengths. Thus, any one of the configurations not included will make a small contribution to the property under consideration. This is not to say that the cumulative effect of omitted configurations may not be significant. However, we do expect to obtain significant quantitative improvement to the HF wave functions by this choice of configurations. At the same time, we retain wave functions of simple and compact form and those for which physical interpretation of key

correlation effects is straightforward.<sup>20</sup>

We have chosen to correlate only the two electrons in the valence shells of the atoms even though the correlation-energy contributions from core orbitals will be larger. We have done this because the valence orbitals overwhelmingly determine the oscillator strengths. Core correlation effects will be indirect, and we expect them to be less significant. We have, for both the initial and final states, constructed all possible symmetry allowed configurations by distributing the two valence electrons into a set of one *s*, one *p*, and one *d* orbital. (For the <sup>1</sup>*P* state of Ba, we also added a *4f* orbital.) Configurations constructed in this way have been described as "internal" configurations.<sup>21</sup> These configurations will have large off-diagonal matrix elements of the Hamiltonian among each other. Further, the diagonal elements are likely to be close in value. Thus, these configurations, as we shall see below, mix strongly with the HF configuration.

The MCHF method is ideally suited to determine wave functions for this choice of configurations. The fact that only a few orbitals are used, in addition to the occupied HF orbitals, means that the MCHF equations do not become much more complicated than the HF equations. To have the maximum benefit from these orbitals it is worthwhile to have them determined by the most reliable method, namely, by the variational method. Our MCHF wave functions were obtained by direct numerical integration of the radial orbital equations that result from the variational method.<sup>17</sup> In this way, we have avoided the problem of the choice of nonlinear parameters of basis functions inherent in analytic expansion self-consistent-field methods.<sup>22</sup> This is of particular advantage for heavy atoms where the optimization of these nonlinear parameters becomes quite tedious.

The nonrelativistic HF wave functions for the ground state of alkaline-earth atoms have the configuration  $(ns)^2\ ^1S$ , where we have suppressed the notations for the core orbitals for brevity. For the ground state, we expect  $(np)^2\ ^1S$  to be the most important configuration to add. The next configuration to add is  $(n'd)^2\ ^1S$ , where  $n' = n - 1$  (except for Mg, where  $n' = n - 3$ ). The three wave functions we used are

$$\Psi_{1c} = (ns)^2 = \text{HF wave function}, \quad (1a)$$

$$\Psi_{2c} = a(ns)^2 + b(np)^2, \quad (1b)$$

$$\Psi_{3c} = a(ns)^2 + b(np)^2 + c(n'd)^2, \quad (1c)$$

where *a*, *b*, and *c* are configuration-mixing coefficients, and  $(ns)^2$ ,  $(np)^2$ , and  $(n'd)^2$  stand for the Slater determinants. The determinants are the <sup>1</sup>*S* components of the indicated configurations for

the valence electrons. Since both the atomic orbitals and the mixing coefficients are allowed to vary in the MCHF method, the  $ns$  and the  $a$ , for instance, in  $\Psi_{2c}$  and  $\Psi_{3c}$  are not identical, though we have used the same symbols for simplicity.

In Table I we present results for the  $^1S$  wave functions of Eqs. (1); namely, total energies, mixing coefficients ( $a, b, c$ ) and expectation values of  $r$  for the  $ns$  orbitals. The energy improvements obtained by adding  $np^2$  and  $n'd^2$  are small, of the order of 1 eV. However, the mixing coefficients, particularly  $b$ , are rather large. Note that the  $\langle r \rangle_{ns}$  are stable as additional configurations are added.

For the lowest  $^1P$  state, the HF configuration is  $(nsnp)$ . In this case, we expect the  $(npn'd)$   $^1P$  configuration to be the most important one to add. We used only two wave functions for the excited state, i.e.,

$$\Phi_{1c} = (nsnp) = \text{HF wave function}, \quad (2a)$$

$$\Phi_{2c} = a'(nsnp) + b'(npn'd), \quad (2b)$$

where  $a'$  and  $b'$  are configuration-mixing coefficients, and  $(nsnp)$  and  $(npn'd)$  denote the Slater determinants which are the  $^1P$  components of the indicated configurations for the valence shells. Again, the MCHF method produces, for instance, different  $ns$  and  $np$  in  $\Phi_{1c}$  and  $\Phi_{2c}$ . Also, orbitals in Eqs. (2) are different from those in the ground state, as is usual. For Ba, we considered also the configuration  $(5d4f)$  as well; i.e.,

$$\Phi_{3c} = a'(6s6p) + b'(6p5d) + c'(5d4f). \quad (2c)$$

This was done first because the  $4f$  shell is next to fill in the Periodic Table. Thus, if this configuration is to be important at all, it should be most important in Ba. Second, the value of  $b'$

TABLE I. Wave-function data for the ground states of alkaline-earth atoms (atomic units). See Eqs. (1) and (3a).

Atom and wave function	Mixing coefficients			Total energy ( $-E_{tot}$ )	$\langle r \rangle$ of the valence $ns$ orbital
	$a$	$b$	$c$		
Mg					
$\Psi_{1c}$	1			199.6146	3.25
$\Psi_{2c}$	0.961	0.275		199.6461	3.20
$\Psi_{3c}$	0.964	0.264	-0.030	199.6469	3.19
Ca					
$\Psi_{1c}$	1			676.7582	4.22
$\Psi_{2c}$	0.953	0.301		676.7851	4.15
$\Psi_{3c}$	0.957	0.283	-0.056	676.7862	4.15
Sr					
$\Psi_{1c}$	1			3131.546	4.63
$\Psi_{2c}$	0.953	0.302		3131.570	4.57
$\Psi_{3c}$	0.958	0.279	-0.071	3131.571	4.56
Ba					
$\Psi_{1c}$	1			7883.545	5.26
$\Psi_{2c}$	0.947	0.320		7883.569	5.19
$\Psi_{3c}$	0.952	0.288	-0.101	7883.569	5.17
$\Psi_r$	1			8128.337	5.08

is so large (-0.64) that we felt that the next term in the CI expansion should be examined.

In Table II we present the data for the  $^1P$  wave functions. Note here that the expectation value  $\langle r \rangle_{np}$  changes significantly as the second configuration is added, contrary to the results for the  $\langle r \rangle_{ns}$  in the ground state. Further, the  $(5d4f)$  configuration for Ba has extremely small weight.

For Ba, we also computed relativistic HF wave functions. The relativistic wave functions are basically the same as the nonrelativistic ones except that the orbitals are four-component spinors, whose radial parts are determined from coupled integro-differential equations.<sup>23</sup> The ground-state wave function is

$$\Psi_r = (ns)^2, \quad (3a)$$

where  $ns \equiv ns_{1/2}$  stands for the relativistic orbital here, in contrast to the nonrelativistic ones in Eqs. (1) and (2).

In the  $jj$ -coupling scheme, the  $(nsnp)$   $^1P_1$  and  $(nsnp)$   $^3P_1$  states cannot be distinguished. Moreover, since  $J=1$  can be obtained by combining  $s_{1/2}$  with either  $p_{1/2} \equiv \bar{p}$  or with  $p_{3/2} \equiv p$ , the  $P_1$  state in the relativistic HF scheme must be represented by a linear combination of  $(nsnp\bar{p})$  and  $(nsnp)$  relativistic configurations, i.e.,

$$\Phi_r = a'(nsnp\bar{p}) + b'(nsnp), \quad (3b)$$

where  $a'$  and  $b'$  are relativistic configuration-mixing coefficients. If we allow free variation of  $a'$  and  $b'$  as well as the orbitals  $ns$ ,  $n\bar{p}$ , and  $np$ , then Eqs. (3b) will represent a relativistic MCHF wave function with  $J=1$ , but the orbital and the spin angular momenta are left unspecified. However, we have fixed the mixing coefficients

TABLE II. Wave-function data for the lowest  $^1P$  states of alkaline-earth atoms (atomic units). See Eqs. (2) and (3b).

Atom and wave function	Mixing coefficients			Total energy ( $-E_{tot}$ )	$\langle r \rangle$ of the valence $np$ orbital
	$a'$	$b'$	$c'$		
Mg					
$\Phi_{1c}$	1			199.4712	6.51
$\Phi_{2c}$	0.976	0.219		199.4821	5.24
Ca					
$\Phi_{1c}$	1			676.6564	7.72
$\Phi_{2c}$	0.898	-0.441		676.6779	5.62
Sr					
$\Phi_{1c}$	1			3131.455	8.34
$\Phi_{2c}$	0.878	-0.479		3131.478	6.09
Ba					
$\Phi_{1c}$	1			7883.468	9.10
$\Phi_{2c}$	0.772	-0.636		7883.501	6.66
$\Phi_{3c}$	0.752	-0.659	-0.036	7883.502	6.63
$\Phi_r$	-0.577	0.816 <sup>a</sup>		8128.256	6 $\bar{p}$ 8.40 6 $p$ 9.30

<sup>a</sup> The coefficients  $a'$  and  $b'$  for the relativistic wave function are those for the  $6s6p_{1/2}$  and  $6s6p_{3/2}$  configurations, respectively. See Eq. (3b).

at  $a' = -\sqrt{\frac{1}{3}}$  and  $b' = \sqrt{\frac{2}{3}}$ , so that the relativistic wave function reduces to the (single configuration)  $^1P$  nonrelativistic case when  $n\bar{p} = np$ . With this choice, the comparison with the nonrelativistic HF results become straightforward. Data from the relativistic wave functions for Ba are included in Tables I and II. Note that the weighted average of  $\langle r \rangle$  for the relativistic  $6\bar{p}$  and  $6p$  orbitals  $[\frac{1}{3}(\langle r \rangle_{6\bar{p}} + 2\langle r \rangle_{6p})]$  is almost the same as that from the nonrelativistic  $6p$  orbital. All wave functions and Slater determinants in Eqs. (1)–(3) are normalized to unity.

The program for the nonrelativistic wave functions is that by Froese-Fischer<sup>17</sup> modified by one of us (P.S.B.). The program for the relativistic wave functions was provided by Desclaux.<sup>18</sup>

### III. GENERALIZED OSCILLATOR STRENGTHS

The generalized oscillator strength is an essential factor in the first Born cross section for inelastic scattering of charged particles in which the target atom is left in an excited state  $n$ :

$$d\sigma_n = \frac{4\pi a_0^2 z^2}{T/\mathfrak{R}} \frac{f_n(K)}{E_n/\mathfrak{R}} d \ln(Ka_0)^2, \quad (4)$$

where  $a_0$  is the Bohr radius,  $\mathfrak{R}$  is the Rydberg energy,  $ze$  is the charge of the incident particle,  $T = \frac{1}{2}mv^2$ ,  $m$  being the *electron* mass (regardless of the type of the incident particle), and  $v$  the speed of the incident particle,  $E_n$  is the excitation energy, and  $\vec{K}\hbar$  is the momentum transfer. The GOS,  $f_n(K)$ , for the excitation of the atom from the initial state  $|0\rangle$  to the final state  $|n\rangle$  is defined as

$$f_n(K) = \frac{E_n}{\mathfrak{R}} \frac{|\langle n | \sum_j e^{i\vec{K} \cdot \vec{r}_j} | 0 \rangle|^2}{(Ka_0)^2}, \quad (5)$$

where  $\vec{r}_j$  is the position vector of the  $j$ th atomic electron, and the summation is over all atomic electrons. Equation (5) reduces to the length form of the dipole oscillator strength in the limit  $K \rightarrow 0$ .

The relativistic expression for the GOS consists of two terms.<sup>24</sup> The first one is due to the Coulomb

TABLE III. Data for the GOS of the resonance transitions in alkaline-earth atoms.

Atoms and wave functions	$f$ [Eq. (6)]	$f'$	First minimum at $(Ka_0)^2 =$	Second maximum at $(Ka_0)^2 =$	$f_n(K)$ at second maximum
Mg					
1c/1c <sup>a</sup>	1.99		3.0	4.4	7.9(-6) <sup>b</sup>
2c/2c	1.71		2.8	4.1	1.5(-5)
2c/3c	1.74	-9.08	2.8	4.1	1.5(-5)
Weiss	1.77				
Zare	1.72				
Expt <sup>c</sup>	1.81				
Ca					
1c/1c	2.26		1.4	2.0	4.7(-5)
2c/2c	1.82		1.5	2.2	1.1(-4)
2c/3c	1.88	-12.99	1.5	2.2	1.2(-4)
Expt	1.75				
Sr					
1c/1c	2.46		1.1	1.5	9.1(-5)
2c/2c	1.95		1.2	1.7	2.0(-4)
2c/3c	2.05	-16.41	1.2	1.7	2.2(-4)
Expt <sup>d</sup>	1.84				
Ba					
1c/1c	2.64		0.77	1.1	1.6(-4)
$r/r$	2.39		0.80	1.2	1.5(-4)
2c/2c	1.70		0.87	1.3	3.2(-4)
2c/3c	1.86		0.88	1.3	3.7(-4)
3c/3c	1.78	-17.00	0.88	1.3	3.8(-4)
Expt	1.59				

<sup>a</sup> For example, 2c/2c stands for the  $\Phi_{2c}/\Psi_{2c}$  combination. The relativistic wave function is denoted by  $r$ .

<sup>b</sup> 7.9(-6) =  $7.9 \times 10^{-6}$ , etc.

<sup>c</sup> Uncertainties in the experimental values quoted in this table are estimated to be ~5% (Refs. 9 and 26).

<sup>d</sup> The experimental  $f$  value of 1.92 for Sr by Lurio *et al.* (Ref. 27) was reduced by 4% to correct for the branching to the lower  $^1D$  state.

interaction between the incident particle and atomic electrons and has the same form as Eq. (5) except that the wave functions are relativistic and the exponential factor is now a  $4 \times 4$  diagonal matrix. It reduces to Eq. (5) in the nonrelativistic limit. The second term is of a relativistic origin and becomes significant only when  $v$  is comparable to the speed of light. Besides, the second term explicitly depends on  $v$  and  $E_n$  in such a way that the GOS is no longer a function of  $K$  alone. For our purpose, the second term is immaterial since it vanishes in the nonrelativistic limit; the relativistic data on Ba given here represent the Coulomb term alone.

To evaluate the GOS and the  $f$  values, we used the valence orbitals only because the main effect of the core orbitals is to reduce the cross section by 1–2% at most through the overlap integrals between the core orbitals of the initial and final states.<sup>18</sup> Experimental values of the excitation energies<sup>25</sup> were used throughout the present work. (Both HF and MCHF excitation energies differ from experimental values by less than 0.5 eV.)

In Table III, the  $f$  values obtained from various wave functions are listed, along with the experimental values. The results obtained using our best wave functions,  $\Phi_{2c}/\Psi_{3c}$  (for Ba  $\Phi_{3c}/\Psi_{3c}$ ), are in reasonable agreement with experiment.<sup>9,26,27</sup> The differences range from 5% for Mg to ~12% for Ba. In contrast, the HF values are considerably poorer. The relativistic effects for Ba (comparing  $1c/1c$  with  $r/r$ ) appear to be of the order of 10% and we expect them to be smaller for the other atoms. We will discuss later the reliability and accuracy of these calculations.

The GOS can be expanded in power series for small momentum transfers,<sup>1</sup> i.e.,

$$f_n(K) = f + f'(Ka_0)^2 + \dots, \quad (6)$$

where  $f' = d f_n(K)/d(Ka_0)^2$  at  $K=0$ . The values of  $f'$  from the  $\Phi_{2c}/\Psi_{3c}$  combination are listed in Table III. (The values of  $f'$  for the alkaline-earth atoms are 20 to 30 times larger than that for the resonance transition of He.<sup>1</sup>) The GOS changes rapidly near the optical limit, and caution is necessary in extrapolating the small-angle electron-impact data (which correspond to small  $K$ ) to obtain or compare with the optical  $f$  values. Since the GOS of higher  $^1P$  transitions in alkaline-earth atoms are expected to have features similar to those in the resonance transitions, the extrapolation of electron-impact experimental data for small angles to the optical limit ( $K \rightarrow 0$ ) should be done with great care.

The GOS for the resonance transitions of alkaline-earth atoms all show a series of zero minima. These minima occur when the matrix ele-

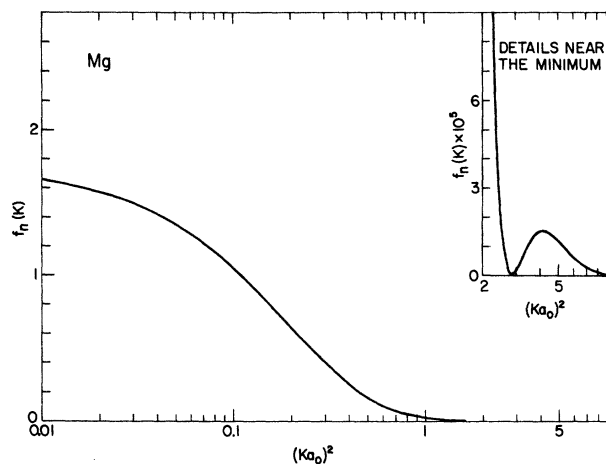


FIG. 1. GOS  $f_n(K)$  for the  $3^1S \rightarrow 3^1P$  transition of Mg as a function of momentum transfer  $\vec{K}\vec{h}$ , obtained from the  $\Phi_{2c}/\Psi_{3c}$  combination (Table III).

ment in the GOS [Eq. (5)] vanishes at certain values of the momentum transfer resulting from a delicate interference of the oscillations in the initial- and final-state wave functions and also in the spherical Bessel function (as a function of  $Kr$ ) that comes from the radial part of the exponential factor in Eq. (5). Hence, the position of a zero minimum is sensitive to details of the wave functions used.

The calculated data on the first minimum and the second maximum (the first maximum is at the optical limit, i.e., at  $K=0$ ) are given also in Table III. The data there show practically no difference between the  $\Phi_{2c}/\Psi_{2c}$  and the  $\Phi_{2c}/\Psi_{3c}$  combinations as far as the extrema are concerned. Figures 1–4 show the GOS calculated from the  $\Phi_{2c}/\Psi_{3c}$  combination with details near the first minima enlarged in the inserts.

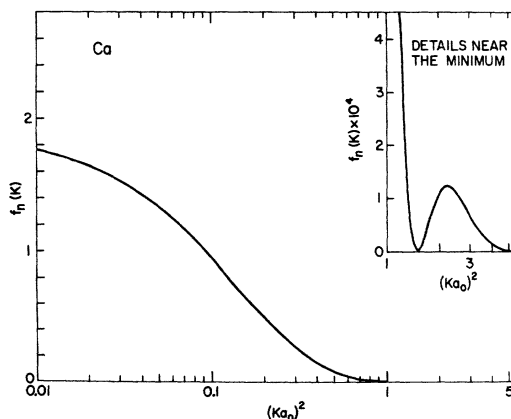


FIG. 2. GOS for the  $4^1S \rightarrow 4^1P$  transition of Ca, obtained from the  $\Phi_{2c}/\Psi_{3c}$  combination (Table III).

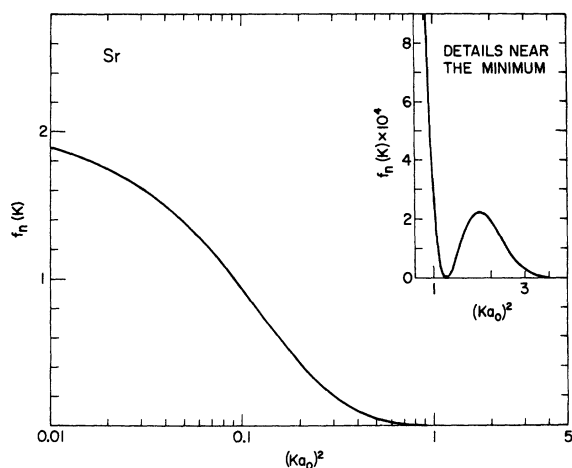


FIG. 3. GOS for the  $5^1S \rightarrow 5^1P$  transition of Sr, obtained from the  $\Phi_{2c}/\Psi_{3c}$  combination (Table III).

Experimental data on the angular distribution of fast electrons inelastically scattered from these atoms would be very valuable in studying the validity of the first Born approximation. At a minimum, all observed intensity must have come from the non-Born effects such as the distortion of the plane waves for the incident and the scattered electron, the electron-exchange effects, distortion of the target charge distributions, etc. Similar minima have been calculated and observed for instance in Xe, Hg, and  $H_2O$  already.<sup>18,28-31</sup> The observed results so far show the first minima at smaller  $K$  values than those predicted from the first Born approximation, and also the observed magnitudes of the second maxima are much larger than the theoretical values. Furthermore, a recent study on the resonance transition of Hg by electron

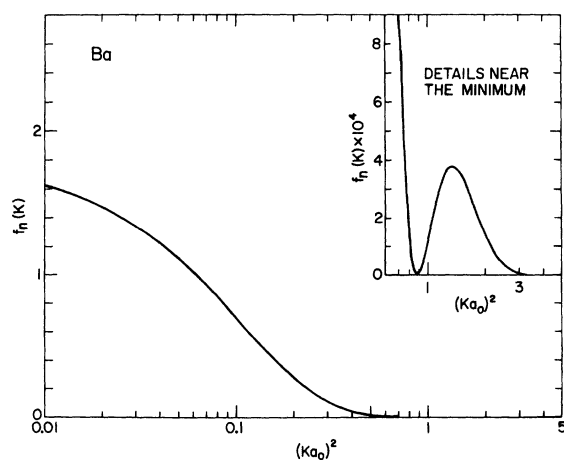


FIG. 4. GOS for the  $6^1S \rightarrow 6^1P$  transition of Ba, obtained from the  $\Phi_{3c}/\Psi_{3c}$  combination (Table III).

impact shows that details of the extrema in the GOS change rapidly as a function of the incident energy.<sup>30,32</sup> The dependence on the incident energy is understandable because it is only in the first Born approximation that the cross section is a function of the momentum transfer alone aside from some trivial factors [see Eq. (4)], i.e., the cross section depends on the incident energy, the excitation energy, and the angle of deflection in a particular combination such that  $K$  is the only variable. The non-Born effects are expected to depend on collision variables in a more complicated manner.

It would be worthwhile to measure the electron-impact cross section for the resonance transition of Ba in particular because the first minimum of the GOS occurs at a rather low  $K$  value (see Table III), i.e., the minimum would occur for moderate incident energies at small angles convenient for experiment.

Now we shall discuss the reliability of the theoretical data presented so far. For Mg, we can compare the  $f$  values calculated from the CI wave functions which include more configurations than ours. Weiss<sup>6</sup> used six configurations for the ground state and four for the excited state, the orbitals being chosen from the occupied and virtual HF orbitals. On the other hand, Zare<sup>33</sup> used the Herman-Skillman orbitals,<sup>34</sup> including eight configurations for the ground state and nine for the excited state. Our  $f$  value from the  $\Phi_{2c}/\Psi_{3c}$  combination agrees very well with those by Weiss and Zare (Table III).

To improve our results further, a substantial number of configurations, including those exciting the core electrons, must be included because we expect that their combined effects would be the same order of magnitude as that from the  $(n'd)^2$  configuration. For Ba, certainly the relativistic effects should also be included at such a stage. At this point, it could be worthwhile to consider approaches alternative to our method; for instance, the core polarization correction proposed by Hameed in which the dipole operator for the optical oscillator strength is modified instead of improving the wave functions themselves.<sup>35</sup>

The drastic changes in the  $f$  values from the  $\Phi_{1c}/\Psi_{1c}$  combination to the  $\Phi_{2c}/\Psi_{2c}$  combination (Table III) are caused by two facts. First, the  $np$  orbital of the  $^1P$  state changes significantly when the second configuration ( $npn'd$ ) is introduced (see  $\langle r \rangle_{np}$  in Table II). Second, the additional configuration  $np^2$  of the ground state introduces a new matrix element between the  $np$  orbital of the ground state and the  $ns$  orbital of the excited state. This matrix element is not only large in magnitude, but it also has a sign opposite

to the dominant matrix element that arises from the HF configurations (between the  $ns$  of the ground state and the  $np$  of the excited state). Our data in Table III indicate that the  $f$  values stabilize more or less once the most important configurations are included in both the initial- and final-state wave functions. The same trend is observed also in the study on the carbon atom by Weiss.<sup>36</sup> The data in this section clearly demonstrate that, for the resonance transitions in alkaline-earth atoms, the Born cross sections computed from the MCHF wave functions with two or three configurations are far superior to those from the (single-configuration) HF wave functions.

#### IV. INTEGRATED BORN CROSS SECTIONS

The integrated cross section is obtained by integrating Eq. (4) over the limits of the momentum transfer,  $K_{\min}$  and  $K_{\max}$ , which are determined from kinematics.<sup>11</sup> This leads to a table of cross sections as a function of incident energies and type of incident particles. Alternatively, the integrated cross section can be expressed in terms of a few parameters when the incident particle is fast<sup>1,10,19</sup>:

$$\begin{aligned} \sigma_n &\equiv \int_{(K_{\min} a_0)^2}^{(K_{\max} a_0)^2} d\sigma_n \\ &= \frac{4\pi a_0^2 z^2}{T/R} [M_n^2 \ln(4c_n T/R) + \gamma_n R/T], \end{aligned} \quad (7)$$

where  $M_n^2 = fR/E_n$ , and the constants  $c_n$  and  $\gamma_n$  are evaluated from the GOS according to Eqs. (12) and (13) of Ref. 1. The constant  $c_n$  depends essentially on the shape of the GOS, while  $\gamma_n$  depends on both the shape and the magnitude of the GOS. The values of  $M_n^2$ ,  $\ln c_n$ , and  $\gamma_n$  evaluated from the  $\Phi_{2c}/\Psi_{3c}$  combination are given in Table IV. To obtain more realistic Born cross section, theoretical  $M_n^2$  may be replaced by experimental values also listed in Table IV. The use of experimental  $M_n^2$  is equivalent to a scaling of the magnitude of the GOS so that its optical limit is given by the experimental  $f$  values. Note that the values of  $\gamma_n$  depend on the mass of the incident particle.

TABLE IV. Parameters for the integrated Born cross section, Eq. (7).<sup>a</sup>

	Mg	Ca	Sr	Ba
$M_n^2$ , theory	5.45	8.74	10.35	10.84
$M_n^2$ , expt	5.67	8.12	9.31	9.66
$\ln c_n$	0.0932	0.582	0.597	0.784
$\gamma_n^{(e)}$	-0.146	-0.242	-0.212	-0.193
$\gamma_n^{(\infty)}$	0.725	0.700	0.811	0.699

<sup>a</sup> Theoretical data for Mg, Ca, and Sr are from the  $\Phi_{2c}/\Psi_{3c}$  combination. The data for Ba are from the  $\Phi_{3c}/\Psi_{3c}$  combination.

For electrons and positrons,  $\gamma_n^{(e)}$  is used, and for heavy particles such as protons and mesons,  $\gamma_n^{(\infty)}$  is appropriate.

Equation (7) should be a good representation of the Born cross section so long as

$$1 \gg \frac{\gamma_n R/T}{M_n^2 \ln(4c_n T/R)}.$$

The values of the constants in Table IV satisfy the above condition even for rather low  $T$  ( $\geq 20$  eV). However, the Born approximation may not be reliable at all at such a low incident energy.

It is difficult to determine the *absolute accuracy* of the Born-cross-section data presented in Table IV. Nevertheless, we can estimate the uncertainties introduced by the use of approximate wave functions in the values of  $\ln c_n$  and  $\gamma_n$  by comparing those from the  $\Phi_{2c}/\Psi_{2c}$  and  $\Phi_{2c}/\Psi_{3c}$  (for Ba, also  $\Phi_{3c}/\Psi_{3c}$ ) combinations. Based on such a comparison, we estimate that the uncertainties  $\ln c_n$

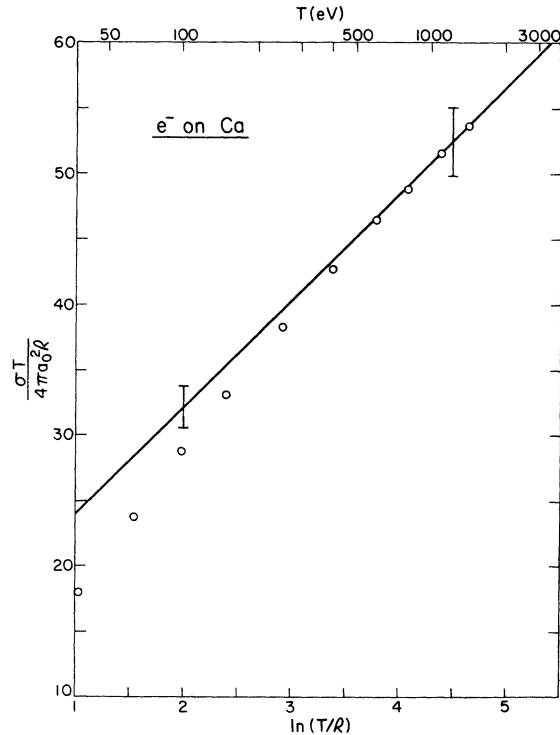


FIG. 5. Fano plot ( $\sigma T$  vs  $\ln T$ ) of the integrated Born cross section (solid line) and the optical excitation function measured by Ehlers and Gallagher (circles, Ref. 37) for the resonance transition of Ca. The Born cross section uses  $M_n^2$  [see Table IV and Eq. (7)] determined from the experimental  $f$  value. The error bars on the Born cross section comes from the 5% uncertainty in the experimental  $f$  value. The relative experimental cross section was normalized to the Born cross section at  $T=1100-1400$  eV. Uncertainties of  $\approx 0.2\%$  are quoted in Ref. 37 for the relative cross section.

and  $\gamma_n$  presented in Table IV should be of the order of 10% or less. Hence, if one uses experimental values of  $M_n^2$  along with theoretical  $\ln c_n$  and  $\gamma_n$  in Eq. (7), the resulting Born cross section for  $T \geq 100$  eV should be accurate (within the limitations of the Born approximation) to whatever the accuracy with which the  $f$  values are known, because  $\ln(4T/R)$  is one order of magnitude larger than  $\ln c_n$  and  $\gamma_n R/T$  for large  $T$ .

Recently, Ehlers and Gallagher<sup>37</sup> measured the optical excitation function for the resonance transition of Ca vapor. In their experiment, the intensity of the light emission corresponding to the  $4^1P \rightarrow 4^1S$  transition is measured after the Ca atoms are bombarded with incident electrons of  $T = 3$ –1400 eV. Ehlers and Gallagher estimate that the effect of cascades from higher states to the  $4^1P$  state is negligible, and hence the Born cross section of Ca in Table IV can be compared directly with the experiment. The experimental data are relative, and we have normalized their data for  $T = 1100$ –1400 eV to the Born cross section. In Fig. 5, we compare the normalized experimental data with the Born cross section. The uncertainty in the relative experimental data indicated in Ref. 37 is  $\sim 0.2\%$ . The departure of the experimental data from the Born cross section below  $T \approx 150$  eV exceeds 6%. We used the experimental  $M_n^2$  value for the Born cross section, but the experimental  $f$  value and therefore the  $M_n^2$  value is known only to  $\sim 5\%$ .<sup>28</sup> Hence, we conclude that the shape of the experimental cross section differs from that of the Born cross section for  $T \lesssim 150$  eV.

## V. CONCLUSIONS

Our results demonstrate that a substantial improvement in the Born cross section for the resonance transitions is achieved by using the MCHF wave functions with one or two more configurations than the HF configuration, both in the ground and excited states. The magnitudes of the mixing coefficients for the  $(np)^2$  configuration for the ground state are  $\sim 0.3$ , and those for the  $(npn'd)$  configuration for the excited state are  $\sim 0.2$ – $0.6$  (Tables I and II).

The GOS near the optical limit changes very rapidly as a function of the momentum transfer [see Eq. (6) and Table III], and this suggests that great care must be taken when extrapolating experimental data on small-angle inelastic scat-

tering to the optical limit to deduce the  $f$  values for the  $^1P$  transitions in alkaline-earth atoms.

The GOS for these resonance transitions show zero minima and hence the (first) Born cross sections vanish at certain values of the momentum transfer. In reality, non-Born effects will dominate in the vicinity of the minima, and therefore, the experimental cross section is not expected to vanish. Experimental study on the minima (e.g., angular distribution of inelastically scattered electrons), particularly their dependence on the incident particle energy, will provide valuable information on the validity of the Born approximations as well as on the magnitudes of higher-order collision effects such as the distortion of the incident plane wave and the charge distribution in the target. Our calculation indicates that the cross section for Ba would have the first minimum near  $(Ka_0)^2 = 0.9$ , or at the deflection angle of  $\approx 9^\circ$  for the incident electron of 500 eV. Judging from other known cases, we expect the experimental minima to occur at smaller values of  $K$  than those listed in Table III for incident electrons of moderate energy.

The parameters for the integrated Born cross sections are given in Table IV. With these parameters, the integrated cross section for arbitrary incident energy ( $T \geq 20$  eV) may be calculated from Eq. (7). The inherent limitations in the Born approximation itself, however, restrict the applicability of Eq. (7) to much higher  $T$ .

The excitation function for the resonance transition of Ca by Ehlers and Gallagher<sup>37</sup> is in excellent agreement (within 5% or better) with our Born cross section for  $T \geq 200$  eV (Fig. 5). To reduce the uncertainties in the theoretical  $f$  values and the GOS to much less than 10%, it would be necessary to include a large number of configurations with excited valence orbitals as well as the core orbitals. Also, relativistic effects should be considered at this point. Such a calculation would lead quickly to complicated numerical procedures, and lose much of its advantages over the conventional CI method.

## ACKNOWLEDGMENTS

We would like to thank Dr. J. P. Desclaux for the use of his relativistic wave-function program, and Dr. A. C. Gallagher for providing us with his experimental data on Ca prior to publication.

\*Work performed under the auspices of the U. S. Atomic Energy Commission.

<sup>1</sup>Y.-K. Kim and M. Inokuti, Phys. Rev. **175**, 176 (1968).

<sup>2</sup>Y.-K. Kim and M. Inokuti, Phys. Rev. **184**, 38 (1969).

<sup>3</sup>K. L. Bell, D. J. Kennedy, and A. E. Kingston, J. Phys. **B 2**, 26 (1969).



- <sup>4</sup>J. van den Bos, *Physica* **42**, 245 (1969).
- <sup>5</sup>D. G. Truhlar, J. K. Rice, A. Kuppermann, S. Trajmar, and D. C. Cartwright, *Phys. Rev. A* **1**, 778 (1970).
- <sup>6</sup>A. W. Weiss, *J. Chem. Phys.* **47**, 3573 (1967).
- <sup>7</sup>Y.-K. Kim and M. Inokuti, *Seventh International Conference on the Physics of Electronic and Atomic Collisions* (North-Holland, Amsterdam, 1971), p. 762.
- <sup>8</sup>Y.-K. Kim and P. S. Bagus, *J. Phys. B* **5**, L193 (1972).
- <sup>9</sup>B. M. Miles and W. L. Wiese, *At. Data* **1**, 1 (1969).
- <sup>10</sup>H. Bethe, *Ann. Phys.* **5**, 325 (1930).
- <sup>11</sup>M. Inokuti, *Rev. Mod. Phys.* **43**, 297 (1971).
- <sup>12</sup>The multiconfiguration Hartree-Fock method was probably first discussed by J. Frenkel, in *Wave Mechanics, Advanced General Theory* (Clarendon, Oxford, England, 1934), Sec. 46.
- <sup>13</sup>D. R. Hartree, W. Hartree, and B. Swirles, *Phil. Trans. R. Soc. Lond.* **A238**, 229 (1939).
- <sup>14</sup>P. S. Bagus, A. Hibbert, and C. Moser, *J. Phys. B* **4**, 1611 (1971), and references therein.
- <sup>15</sup>P. S. Bagus and J. Bauche, *Phys. Rev. A* (to be published).
- <sup>16</sup>J. P. Desclaux, *Intern. J. Quant. Chem. Symposium No. 6*, 25 (1972).
- <sup>17</sup>C. Froese-Fischer, *Comp. Phys. Commun.* **1**, 151 (1970).
- <sup>18</sup>Y.-K. Kim, M. Inokuti, G. E. Chamberlain, and S. R. Mielczarek, *Phys. Rev. Lett.* **21**, 1146 (1968).
- <sup>19</sup>W. F. Miller and R. L. Platzman, *Proc. Phys. Soc. (Lond.)* **A70**, 299 (1957).
- <sup>20</sup>P. S. Bagus, A. J. Freeman, and F. Sasaki, *Phys. Rev. Lett.* **30**, 850 (1973).
- <sup>21</sup>H. J. Silverstone and O. Sinanoğlu, *J. Chem. Phys.* **44**, 1899 (1966).
- <sup>22</sup>C. C. J. Roothaan and P. S. Bagus, in *Methods in Computational Physics* (Academic, New York, 1963), Vol. II, p. 47.
- <sup>23</sup>Y.-K. Kim, *Phys. Rev.* **154**, 17 (1967).
- <sup>24</sup>U. Fano, *Ann. Rev. Nucl. Sci.* **13**, 1 (1963), Sec. 2. 3.
- <sup>25</sup>C. E. Moore, *Natl. Bur. Stand. Circ. No. 467*, Vol. I-III (1949-1958).
- <sup>26</sup>For experimental data on Mg and Ca, see W. L. Wiese, M. W. Smith, and B. M. Miles, *Atomic Transition Probabilities*, *Natl. Bur. Stand. Ref. Data Series No. 22* (U.S. GPO, Washington, D. C., 1969), Vol. II.
- <sup>27</sup>For experimental data on Sr see A. Lurio, R. L. deZafra, and R. J. Goshen, *Phys. Rev.* **134**, A1198 (1964).
- <sup>28</sup>A. Skerbele and E. N. Lassette, *J. Chem. Phys.* **58**, 2887 (1973).
- <sup>29</sup>J. C. McConnell, Ph.D. thesis (Queen's University of Belfast, 1969) (unpublished).
- <sup>30</sup>F. Hanne and J. Kessler, *Phys. Rev. A* **5**, 2457 (1972).
- <sup>31</sup>K. J. Miller, S. R. Mielczarek, and M. Krauss, *J. Chem. Phys.* **51**, 26 (1969).
- <sup>32</sup>D. H. Madison and W. N. Shelton, *Phys. Rev. A* **7**, 514 (1973).
- <sup>33</sup>R. N. Zare, *J. Chem. Phys.* **47**, 3561 (1967).
- <sup>34</sup>F. Herman and S. Skillman, *Atomic Structure Calculations* (Prentice Hall, Englewood Cliffs, N.J., 1963).
- <sup>35</sup>S. Hameed, *J. Phys. B* **5**, 746 (1972).
- <sup>36</sup>A. W. Weiss, *Phys. Rev.* **162**, 71 (1967).
- <sup>37</sup>V. J. Ehlers and A. C. Gallagher, *Phys. Rev. A* **7**, 1573 (1973).